

Bounds for rotating convection at infinite Prandtl number from semidefinite programs

A. Tilgner 

Institute of Astrophysics and Geophysics, University of Göttingen, Friedrich-Hund-Platz 1, 37077 Göttingen, Germany



(Received 24 April 2022; accepted 30 August 2022; published 16 September 2022)

Bounds for the poloidal and toroidal kinetic energies and the heat transport are computed numerically for rotating convection at infinite Prandtl number with both no-slip and stress-free boundaries. The constraints invoked in this computation are linear or quadratic in the problem variables and lead to the formulation of a semidefinite program. The bounds behave as a function of Rayleigh number at fixed Taylor number qualitatively in the same way as the quantities being bounded. The bounds are zero for Rayleigh numbers smaller than the critical Rayleigh number for the onset of convection, they increase rapidly with Rayleigh number for Rayleigh numbers just above onset, and increase more slowly at large Rayleigh numbers. If the dependencies on Rayleigh number are approximated by power laws, one obtains larger exponents from bounds on the Nusselt number for Rayleigh numbers just above onset than from the actual Nusselt number dependence known for large but finite Prandtl number. The wavelength of the linearly unstable mode at the onset of convection appears as a relevant length scale in the bounds.

DOI: [10.1103/PhysRevFluids.7.093501](https://doi.org/10.1103/PhysRevFluids.7.093501)

I. INTRODUCTION

The optimum theory of turbulence attempts to replace the exact computation of time-averaged global quantities, such as the heat transfer across a convecting layer, by a simpler calculation at the price of obtaining only upper bounds to the quantities of interest. The method most frequently used for this purpose is the background field method [1–4], which is more convenient to use but which ultimately produces the same results as another method based on Refs. [5–7], at least for the convection problem [8]. Both classes of methods do not make use of the full Navier-Stokes equation but use relations derived from integrals of this equation, such as the energy budget. As a consequence, a major disadvantage of these methods applied to convection flows is that they are insensitive to the presence of the Coriolis term in the momentum equation. Rotational effects appear in the bounds derived from straightforward optimum theory of convection only for reduced sets of equations [9,10], the simplest representative of which is the model of the infinite Prandtl number.

Rotating convection is a problem with many applications in geophysics and astrophysics. In this context, convection at large Prandtl numbers in particular also plays a role. Solutal convection in the oceans or in planetary cores [11] is characterized by Prandtl numbers around 10^3 or 10^4 . It is not obvious if, or under which conditions, rotating convection with Prandtl numbers this large behaves the same as convection in a fluid of infinite Prandtl number. However, these applications motivate the study of convection at infinite Prandtl number as a simple limiting case. In addition, it was recently shown [12] how bounds derived for infinite Prandtl number convection can be used as a starting point for the computation of bounds for arbitrary Prandtl number. This calculation can be summarized as a background field method with a background field for velocity, which is not fixed in advance and time independent, but which instead is the solution of the momentum equation for

infinite Prandtl number. The bounds derived in this manner for general Prandtl number cannot be lower than the bounds for infinite Prandtl number. It is therefore interesting to explore numerically which are the best possible bounds derivable at infinite Prandtl number from the constraints used in optimum theory of turbulence as we presently know it.

The known bounds derived by analytical means [12–14] for the heat transfer in rotating infinite Prandtl number convection are too loose to be satisfactory. While these bounds qualitatively reproduce a reduction of the heat transport by rotation, they do not restrict the advective heat transfer to zero for Rayleigh numbers below the critical Rayleigh number computed from linear stability analysis.

A numerical computation of upper bounds for heat transfer in rotating convection at infinite Prandtl number with stress-free boundaries previously appeared in Ref. [15]. The parameter range covered in that study is too small to allow us to really judge the performance of the bounds by comparing them with experimental data. We also know from the nonrotating problem that the optimum theory for infinite Prandtl number behaves very differently for stress-free and no-slip boundaries [16,17], and the boundary conditions relevant for experiments are no-slip rather than stress-free boundaries. Finally, Ref. [15] did not compute bounds on energies.

There are thus several motivations to revisit the problem of determining numerically the optimal bounds for rotating convection at infinite Prandtl number. The computation presented here makes use of the same constraints as previous work. These constraints only include linear and quadratic terms. This problem can be cast in the form of a semidefinite program (SDP). Numerical techniques of SDP have already been applied to convection problems [18,19] and they promise to be more generally applicable to bounding hydrodynamic quantities [4,20]. The SDP implemented for rotating convection at infinite Prandtl number is explained in the next section, and the results are presented in Sec. III.

II. SEMIDEFINITE PROGRAM

We consider a plane layer infinitely extended in the x and y directions and of thickness h with bounding planes perpendicular to the z axis in a frame of reference rotating with angular velocity Ω about the z axis. The gravitational acceleration acts in the direction of negative z . The layer is filled with fluid of density ρ , kinematic viscosity ν , thermal diffusivity κ , and thermal expansion coefficient α . Top and bottom boundaries are held at the fixed temperatures T_{top} and $T_{\text{top}} + \Delta T$, respectively. Within the Boussinesq approximation, there are in general three control parameters: the Prandtl, Rayleigh, and Taylor numbers Pr , Ra , and Ta defined as

$$\text{Pr} = \frac{\nu}{\kappa} \quad \text{Ra} = \frac{g\alpha\Delta T h^3}{\kappa\nu} \quad \text{Ta} = \frac{4\Omega^2 h^4}{\nu^2}. \quad (1)$$

Here, we immediately specialize to the limit of infinite Pr in which case the equations of evolution may be written as follows in terms of the nondimensional fields of velocity $\mathbf{v}(\mathbf{r}, t)$, pressure $p(\mathbf{r}, t)$, and temperature deviation from the conductive temperature profile $\theta(\mathbf{r}, t)$ where $\theta(\mathbf{r}, t) = T(\mathbf{r}, t) - 1 + z$ with $T(\mathbf{r}, t)$ being the temperature:

$$\sqrt{\text{Ta}}\hat{z} \times \mathbf{v} = -\nabla p + \text{Ra}\theta\hat{z} + \nabla^2 \mathbf{v} \quad (2)$$

$$\partial_t \theta + \mathbf{v} \cdot \nabla \theta - v_z = \nabla^2 \theta \quad (3)$$

$$\nabla \cdot \mathbf{v} = 0. \quad (4)$$

\hat{z} denotes the unit vector in z direction. The conditions at the boundaries $z = 0$ and $z = 1$ on the temperature imply that $\theta = 0$ there. Both stress-free and no-slip conditions will be investigated. At stress-free boundaries, $\partial_z v_x = \partial_z v_y = v_z = 0$, whereas $\mathbf{v} = 0$ on no-slip boundaries. Periodic boundary conditions are assumed in the horizontal directions with arbitrary periodicity lengths.

We now decompose \mathbf{v} into poloidal and toroidal scalars ϕ and ψ such that $\mathbf{v} = \nabla \times \nabla \times (\phi \hat{\mathbf{z}}) + \nabla \times (\psi \hat{\mathbf{z}})$, which automatically fulfills $\nabla \cdot \mathbf{v} = 0$. An additional term with a mean flow is not necessary at infinite Prandtl number [12]. The z component of the curl and the z component of the curl of the curl of Eq. (2) yield the equations of evolution for ϕ and ψ ,

$$\sqrt{\text{Ta}} \partial_z \Delta_2 \psi = \nabla^2 \nabla^2 \Delta_2 \phi - \text{Ra} \Delta_2 \theta \quad (5)$$

$$-\sqrt{\text{Ta}} \partial_z \Delta_2 \phi = \nabla^2 \Delta_2 \psi \quad (6)$$

with $\Delta_2 = \partial_x^2 + \partial_y^2$. The boundary conditions become $\phi = \partial_z^2 \phi = \partial_z \psi = 0$ for stress-free boundaries and $\phi = \partial_z \phi = \psi = 0$ for no-slip boundaries.

The Eqs. (5) and (6) determine ϕ and ψ , and hence \mathbf{v} , in dependence of θ . The equations of evolution (2)–(4) therefore reduce to the single equation (3) in which \mathbf{v} ultimately is some function of θ . Since there is no closed expression for this function, we keep the variables ϕ , ψ and \mathbf{v} in subsequent formulas bearing in mind that they are nothing but functions of θ .

We next define averages over space of a function $f(\mathbf{r})$ and over time of a function $g(t)$ with the symbols

$$\overline{f(t)} = \lim_{\tau \rightarrow \infty} \frac{1}{\tau} \int_0^\tau f(t) dt \quad \langle g(\mathbf{r}) \rangle = \frac{1}{V} \int g(\mathbf{r}) dV, \quad (7)$$

where V is the volume of a periodicity volume. The product of Eq. (3) with θ followed by a volume average leads in this notation to

$$\partial_t \langle \frac{1}{2} \theta^2 \rangle = \langle v_z \theta \rangle - \langle |\nabla \theta|^2 \rangle. \quad (8)$$

The quantities for which we will seek bounds in this paper are the time- and volume-averaged heat transport $\langle \overline{v_z \theta} \rangle$, the poloidal energy

$$E_{\text{pol}} = \left\langle \frac{1}{2} |\nabla \times \nabla \times (\phi \hat{\mathbf{z}})|^2 \right\rangle \quad (9)$$

and the toroidal energy

$$E_{\text{tor}} = \left\langle \frac{1}{2} |\nabla \times (\psi \hat{\mathbf{z}})|^2 \right\rangle. \quad (10)$$

It only makes sense to ask for bounds on energy in convection with stress-free boundaries if one specifies a certain frame of reference because any solution to the equations of evolution may be transformed to another solution with stress-free boundary conditions simply by changing to another frame of reference moving at an arbitrarily large horizontal translation velocity. We adopt the same convention as in Ref. [12] and select the frame of reference in which total momentum is zero.

The method to find these bounds is exactly the same as in Ref. [18]. The only difference in the numerical implementation is that in the nonrotating problem of Ref. [18], the toroidal scalar ψ was always zero, whereas here, both ϕ and ψ have to be computed in terms of θ taking into account a Ta different from zero. The principle of the method is summarized here to make the paper self-contained.

We select test functions $\varphi_n(z)$, $n = 1 \dots N$, which depend on z only and project onto them the temperature equation (3):

$$\partial_t \langle \varphi_n \theta \rangle = \langle \varphi_n \partial_z (\theta \Delta_2 \phi) \rangle + \langle \varphi_n \nabla^2 \theta \rangle. \quad (11)$$

We now build a functional $G(\lambda_1 \dots \lambda_N, \lambda_R, \theta)$ as a linear combination of the right-hand sides of Eqs. (11) and (8):

$$G(\lambda_1 \dots \lambda_N, \lambda_R, \theta) = \sum_{n=1}^N \lambda_n [\langle \varphi_n \partial_z (\theta \Delta_2 \phi) \rangle + \langle \varphi_n \nabla^2 \theta \rangle] + \lambda_R [\langle \theta \Delta_2 \phi \rangle + \langle |\nabla \theta|^2 \rangle]. \quad (12)$$

Let us call Z the function for whose time average we want to find a bound. For example, $Z = \langle v_z \theta \rangle$ if we want to compute a bound for the heat transport. Z is a quadratic functional of θ for the problems

of bounding heat transport, E_{pol} and E_{tor} . Let us suppose we know a number λ_0 and Lagrange multipliers $\lambda_1 \dots \lambda_N, \lambda_R$ such that all fields $\theta(\mathbf{r})$ obeying the boundary conditions for θ satisfy the following inequality:

$$-Z + \lambda_0 + G(\lambda_1 \dots \lambda_N, \lambda_R, \theta) \geq 0. \quad (13)$$

If we take the time average of this inequality keeping in mind that G is a linear combination of expressions equal to a time derivative, we find $\bar{Z} \leq \lambda_0$.

The argument may equally well be recast in the form of a background method or in terms of an auxiliary function [4]. If we call $\varphi(z) = \sum_{n=1}^N \lambda_n \varphi_n(z)$, we may write G as

$$G(\lambda_1 \dots \lambda_N, \lambda_R, \theta) = \langle \varphi \partial_t \theta \rangle - \lambda_R \partial_t \left\langle \frac{1}{2} \theta^2 \right\rangle = -\frac{\lambda_R}{2} \frac{d}{dt} \left\langle \left(\theta - \frac{\varphi(z)}{\lambda_R} \right)^2 \right\rangle \quad (14)$$

so that the background field $\tau(z)$ used within the background field method applied to convection [3] is identical with [18] $1 - z + \varphi(z)/\lambda_R = \tau(z)$.

The best possible bound on \bar{Z} is obtained by minimizing λ_0 over the $\lambda_1 \dots \lambda_N, \lambda_R$ subject to the constraint (13). This optimization problem turns into an SDP after discretization of θ . The computations presented here discretized θ with N Chebyshev polynomials in z and a Fourier decomposition in x and y . Resolutions with N up to 512 were used. The package `cvxopt` provided the numerical solutions of the SDP. The details of the numerical code will not be described here as they are exactly the same as in Ref. [18]. The technical points explained in this reference are the symmetry of the problem about $z = 1/2$, an automated search for an active set of wave numbers in the Fourier decomposition in the horizontal plane, the exact formulation of the boundary conditions on θ , a partial integration of Eq. (12) and a rescaling of λ_0 with powers of Ra .

The result is an SDP, which yields the desired optimal bound, but it is not completely straightforward to compare the optimal coefficients λ_n to the optimal $\varphi(z)$ or $\tau(z)$ one might obtain from an analytical calculation. The reason for this is that the optimization problem includes constraints containing the integral of two functions $f(z)$ and $g(z)$, one of which (for example f) is replaced in the course of the discretization by a sum of Dirac δ functions as $\sum_{n=1}^N f_n \delta(z - z_n)$ where the collocation points z_n are given by

$$z_n = \frac{1}{2} \left[1 + \cos \left(\pi \frac{n-1}{N-1} \right) \right] \quad n = 1 \dots N. \quad (15)$$

The integral $\int f(z)g(z)dz$ then becomes the sum $\sum_{n=1}^N f_n g(z_n)$. There is no immediate relationship between $f(z)$ and the f_n if the f_n are chosen such that the sum $\sum_{n=1}^N f_n g(z_n)$ approximates as closely as possible the integral $\int f(z)g(z)dz$. For instance, these f_n depend on the resolution N and the collocation points z_n . The SDP as implemented returns a set of coefficients a_n , which appear in a representation of the first derivative of $\varphi(z)$ as $\varphi'(z) = \sum_{n=1}^N a_n \delta(z - z_n)$. The magnitude of these a_n is not directly connected to optimal background fields obtained from analytical calculations, but the general dependence on space must be comparable.

Analytical treatment of infinite Prandtl number convection with the background field method [13,14,16,21] used functions $\tau(z)$ or $\varphi(z)$ whose first derivative is either constant or piecewise constant, with a certain value for this derivative in the central region of the layer and another value in two boundary layers adjacent to the top and bottom boundaries. More sophisticated background fields were also used in the nonrotating problem [22,23]. The thickness of the boundary layers is imposed by the Rayleigh number. Figure 1 shows for a few examples the a_n , each a_n plotted at the location z_n . The a_n are approximately constant for the z_n near the center of the layer, but there is a rapid variation of the a_n within apparent boundary layers. More than one extremum appears for no-slip boundaries at large Ta . The thickness of the boundary layer for no-slip boundaries, defined from the location of the minimal a_n , is compatible with the scaling in $\text{Ta}^{-1/4}$ known from Ekman layers, whereas the layers remain thicker for free-slip boundary conditions. The demand on resolution is therefore higher for no-slip boundaries.

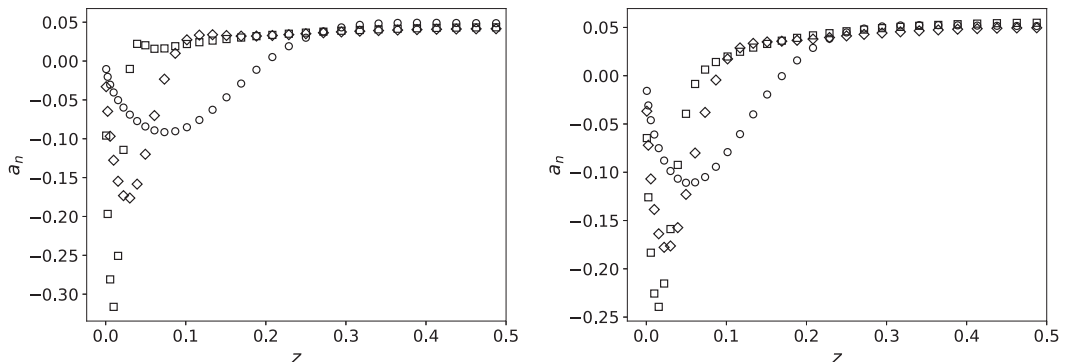


FIG. 1. Coefficients a_n , plotted at locations z_n , for $Ta = 10^4$ (circles), 10^6 (diamonds), and 10^8 (squares) and a resolution $N = 64$. The boundary conditions are no slip (left panel) and stress free (right panel). The Rayleigh number is in all cases approximately 4 times critical: $Ra = 34.92Ta^{2/3}$.

III. RESULTS

The bound H on the advective heat transport is obtained from the selection $Z = \langle v_z \theta \rangle$. The results of experiments or numerical simulations are usually reported in terms of the Nusselt number, which is identical to $\overline{\langle v_z \theta \rangle} + 1$. For easier comparison, Fig. 2 shows $H + 1$ as a function of Ra for various Ta . The graphs have the general appearance familiar from experiments or numerical simulations: the bound H is exactly zero for Ra less than the critical Rayleigh number Ra_{crit} computed from linear stability analysis and the heat transport is reduced by rotation compared with the nonrotating flows at Rayleigh numbers just above onset with a rapid increase of $H + 1$ as a function of Ra , whereas at sufficiently large Ra , $H + 1$ increases more slowly as a function of Ra at a rate asymptotically identical with the nonrotating case. For no-slip boundaries, there is an overshoot in the sense that the bound for rotating convection is actually larger than that for the nonrotating case in an intermediate interval of Ra . This echoes the behavior known from experiments and simulations in which the Nusselt number of rotating convection may exceed the Nusselt number of nonrotating convection [25–27], a behavior that is not observed for stress-free boundaries [28].

There does not seem to be any numerical data available for strictly infinite Pr , but the results in Ref. [29] suggest that there is no significant difference in the Nusselt number in going from $Pr = 7$ to $Pr = 100$ so that it is meaningful to compare data obtained for Pr equal to 7 or larger to the bounds for infinite Pr . The bounds for no-slip boundaries in Fig. 2 may then directly be compared to the data compiled in Fig. 1 of Ref. [30]. It is frequently attempted to fit power laws to experimentally or numerically determined values of the Nusselt number. Power laws are not a terribly good fit to either H or the bounds $H + 1$ in Fig. 2 in the rotation dominated regime, but if one insists on fitting power laws to the dependence of $H + 1$ on Ra , one finds for no-slip boundaries exponents of 2, 3.5, and 4.5 at approximately the Taylor numbers at which the exponents for the actual Nusselt number at $Pr = 7$ are 1.2, 3, and 3.6 according to Ref. [30]. The bounds parallel the behavior of the Nusselt number in that larger exponents are necessary at larger Ta , but the exponents obtained from fits to the bounds are systematically larger than those obtained from the experiments.

For free-slip boundaries, the dependence of $H + 1$ on Ra for Ra just above Ra_{crit} is reasonably fitted by $H + 1 = (Ra/Ra_{\text{crit}})^2$ at all Ta . From simulations [27] at $10^2 \lesssim Ta \lesssim 10^8$ one finds for $Pr = 7$ that the Nusselt number just above onset behaves approximately as $(Ra/Ra_{\text{crit}})^{6/5}$, so that the exponents fitting the bounds again appear to be larger than what they should be if the bounds were sharp.

It is also seen in Figs. 1 and 2 that for stress-free boundaries, the nonrotating behavior is attained only at very large Rayleigh numbers, if at all. For infinite Pr , it is not obvious why the behavior of

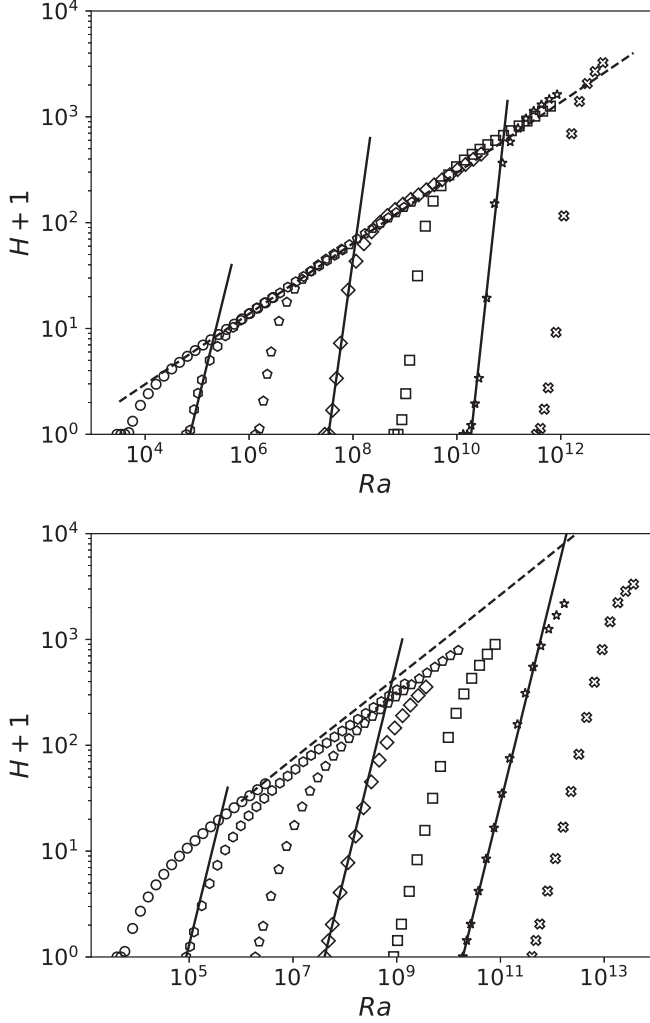


FIG. 2. The bound on the Nusselt number $H + 1$ as a function of Ra for $Ta = 10^4$ (circles), 10^6 (hexagons), 10^8 (pentagons), 10^{10} (diamonds), 10^{12} (squares), 10^{14} (stars), and 10^{16} (crosses). The top panel is for no slip boundaries and the bottom panel for stress free boundaries. The dashed lines are fits to bounds obtained for $Ta = 0$ (see Refs. [17,18]) given by $H + 1 = 0.101 \times Ra^{0.4} + 0.70965 \times Ra^{0.2} - 7.166$ for stress-free boundaries and $H + 1 = 0.139 \times Ra^{1/3}$ for no-slip boundaries. The continuous lines show functions of the form $(Ra/Ra_{\text{crit}})^\beta$ with Ra_{crit} computed from the asymptotically valid expression [24] $Ra_{\text{crit}} = 8.73 \times Ta^{2/3}$ for stress-free boundary conditions (top panel) and obtained as part of the fitting procedure for no-slip boundary conditions (bottom panel). The exponent β in the case of no-slip boundaries is 3 ($Ta = 10^6$), 3.5 ($Ta = 10^{10}$), and 4.5 ($Ta = 10^{14}$), whereas $\beta = 2$ for all lines drawn for stress-free boundaries.

rotating and nonrotating convection should approach each other at any Ra . We currently do not have a solid understanding of the mechanism that determines the transition from convection dominated by Coriolis force to convection nearly independent of rotation as Ra is increased. King *et al.* [29] suggested that the transition occurs when the Ekman layer and thermal boundary layer are equally thick. However, this criterion cannot be generally applicable because the same transition is observed for stress-free and for no-slip boundary conditions [27,28] and there are no Ekman layers near the stress-free boundaries. The most intuitive criterion is based on the Rossby number. If this number

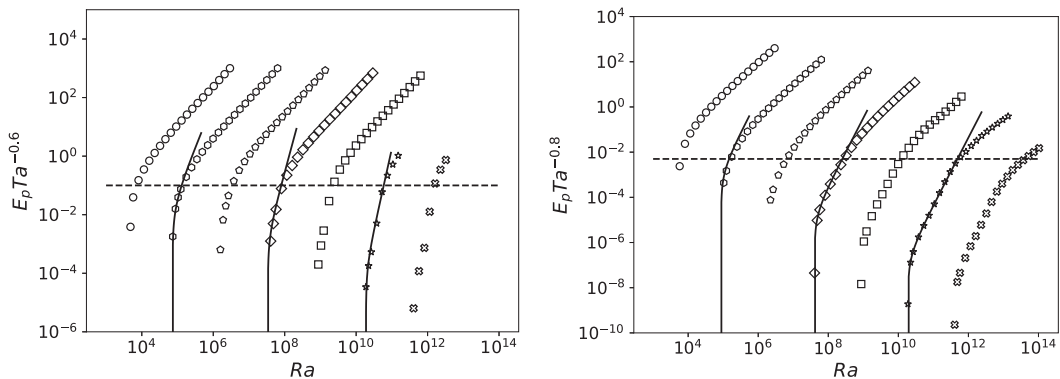


FIG. 3. The bound E_p on the poloidal energy shown in the combination $E_p Ta^{-0.6}$ for no-slip boundaries (left panel) and $E_p Ta^{-0.8}$ for stress-free boundaries (right panel) with the same symbols as in Fig. 2. The continuous lines indicate the functions $(Ra/Ra_{\text{crit}})[(Ra/Ra_{\text{crit}})^\beta - 1]Ta^{1/3}$ for $\beta = 2, 3.5,$ and 4.5 in the left panel and $\beta = 2$ in the right panel. The dashed horizontal lines are located at $E_p Ta^{-0.6} = 0.1$ (left panel) and $E_p Ta^{-0.8} = 5 \times 10^{-3}$ (right panel).

is large, the Coriolis term is small compared with the advection term in the momentum equation. Horn and Shishkina [31] classified states of rotating convection with the help of the Rossby number based on the free-fall velocity, $(g\alpha\Delta Th)^{1/2}/(\Omega h) \propto (Ra/(\text{Pr}Ta))^{1/2}$. This number is always zero in the model of convection at infinite Prandtl number, which is not surprising because there is no advection term left in the momentum equation compared to which the Coriolis term could be small. It is also known [27,28] that if the Rossby number is based on the actual flow velocity rather than the free-fall velocity, the Rossby number does not allow one to distinguish at $\text{Pr} = 0.7$ or $\text{Pr} = 7$ between convection dominated by rotation from convection nearly independent of rotation. The balance between Coriolis and rotation terms does not seem to be essential for the transition.

Another reasoning, put forward by Schmitz and Tilgner [28], combines the asymptotic behavior of the Nusselt number at small and large Ra for fixed Ta to predict that the transition should occur if

$$(E_{\text{pol}} + E_{\text{tor}})Ta^{-1} = \text{const.} \quad (16)$$

This criterion, which is valid for both types of boundary conditions [27], is independent of Pr and can be immediately extended to infinite Pr . This criterion also motivates the form in which the bounds are presented in the following two figures.

Figures 3 and 4 show the bounds on poloidal and toroidal energies, E_p and E_t , obtained from $Z = \langle \frac{1}{2} |\nabla \times \nabla \times (\phi \hat{z})|^2 \rangle$ and $Z = \langle \frac{1}{2} |\nabla \times (\psi \hat{z})|^2 \rangle$, respectively. At any Ta , these bounds show again two regions of Ra in which rotation is either suppressing convection or not. To better identify the interval of Ra dominated by rotation, it helps to make a connection with the bounds on the heat transport. The z component of velocity is zero at the boundaries so that the bound H implies by virtue of the Poincaré inequality a bound on the poloidal energy [18] as

$$E_{\text{pol}} \leq \frac{1}{2\pi^2} RaH. \quad (17)$$

However, one expects a stricter bound to be valid. Taking the dot product of the momentum equation (2) with \mathbf{v} and integrating over space leads to

$$\sum_{ij} \langle (\partial_j v_i)^2 \rangle = Ra \langle v_z \theta \rangle. \quad (18)$$

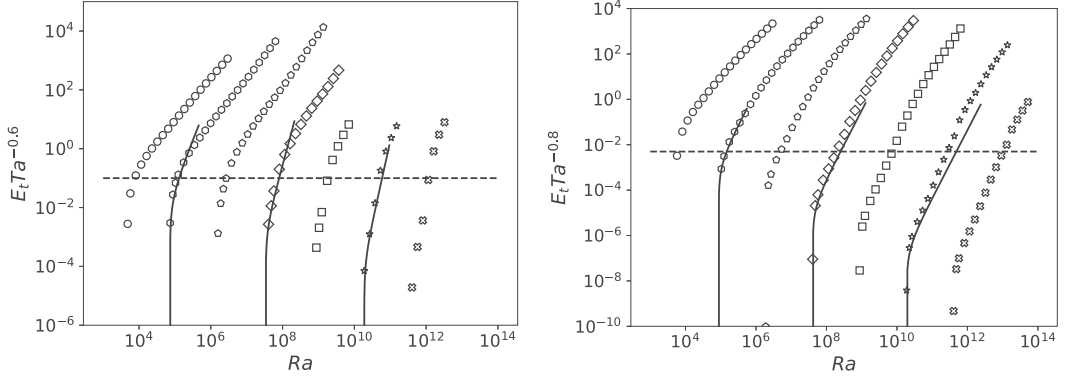


FIG. 4. The bound on the toroidal energy, E_t , in the same representation as E_p in Fig. 3, with the same symbols and the same dashed and continuous lines. The left panel is for no slip boundaries and the right panel for stress-free boundaries.

If λ_c is a characteristic length scale of the flow, one expects $\sum_{ij} \langle (\partial_j v_i)^2 \rangle \sim (E_{\text{pol}} + E_{\text{tor}}) / \lambda_c^2$ and therefore $E_{\text{pol}} \leq \text{Ra}H / \lambda_c^2$. At Ra just above critical, the typical length scale of rotation is the wavelength of the most unstable mode in linear stability analysis, which leads to [24] $\lambda_c^2 \propto \text{Ta}^{-1/3}$. Replacing H by its power-law fit deduced from Fig. 2 and using $\text{Ra} / \text{Ra}_{\text{crit}}$ as variable, one expects the existence of a bound E_p of the form

$$E_{\text{pol}} \leq E_p \propto \frac{\text{Ra}}{\text{Ra}_{\text{crit}}} \left[\left(\frac{\text{Ra}}{\text{Ra}_{\text{crit}}} \right)^\beta - 1 \right] \text{Ta}^{1/3}. \quad (19)$$

This functional form, with a prefactor equal to 1, fits well the dependence of E_p on Ra for rotating convection with both types of boundary conditions and Ra close to Ra_{crit} . The bound E_p obtained from the SDP is therefore sensitive to the variation of the characteristic length scale of convection with Ta , in agreement with analytically computed bounds [12].

Equation (19) fails to be a good fit if Ra is large enough, which marks the upper edge of the interval of Ra in which the bound E_p is controlled by the Coriolis force. Figure 3 shows that the bound on E_{pol} is indicative of rapidly rotating convection only if $E_p \text{Ta}^{-0.6} \leq 0.1$ for no slip and $E_p \text{Ta}^{-0.8} \leq 5 \times 10^{-3}$ for stress-free boundaries. Figure 4 repeats all the previous considerations for the toroidal energy. For no-slip boundaries, the same function as in Eq. (19) approximates also the bounds for the toroidal energy in the rapidly rotating regime, which implies near equipartition between the poloidal and toroidal energies in as far as bounds are concerned. In the case of stress-free boundaries, the bound on toroidal energy E_t exceeds the bound on poloidal energy. For both boundary conditions, E_t exceeds E_p in the high Rayleigh number regime even though the toroidal energy is zero in the nonrotating case. At finite Pr , simulations [31] show that the fraction of toroidal to total energy decreases with Ra at large Ra . This behavior is not reproduced by the bound E_t , possibly because Eq. (6) prevents the fraction of toroidal to total energy from decreasing to zero, which would mean that in this particular respect, rotating convection at infinite and finite Pr are fundamentally different from each other. Figure 4 also shows that for no-slip boundaries, the condition $E_t \text{Ta}^{-0.6} \leq \text{const.}$ reasonably delimits the region in parameter space in which the bound E_t is determined by the length scale of rapidly rotating convection near onset, λ_c . Combined with the bounds for poloidal energy, this leads to $(E_p + E_t) \text{Ta}^{-0.6} \leq \text{const.}$ as a criterion for the bounds being mainly controlled by the Coriolis term, which contains a different exponent than Eq. (16).

IV. SUMMARY

Predictions of heat transport in turbulent convection necessarily rely on empirically motivated assumptions. An early approach assumed that the thermal boundary layers are marginally stable which leads in the nonrotating case to [32,33] $\text{Nu} \propto \text{Ra}^{1/3}$. It is possible to derive bounds that come at least to within logarithmic factors of $\text{Ra}^{1/3}$ for convection at infinite Prandtl number [17,21–23,34]. Bounds for convection at arbitrary Prandtl number [3] are no better than $\text{Nu} \propto \text{Ra}^{1/2}$. It is tempting to ascribe this difference to the different nature of the equations of evolution: the momentum equation becomes a diagnostic equation at infinite Pr, effectively reducing the problem to a single equation for the temperature field. It is then interesting to investigate whether similarly tight bounds can be derived for rotating convection at infinite Pr.

Attempts at analytically deriving bounds on heat transport in rotating convection at infinite Pr have been based on the background field method [13,14], which enforces constraints derived from the surface average over horizontal planes of the temperature equation and the volume average of the temperature equation multiplied by θ . The numerical search of an optimal bound satisfying constraints of this form leads to an SDP. For $\text{Ta} = 0$ and no-slip boundaries, the SDP technique finds an upper bound for the heat transport, which varies as a function of Ra as $\text{Ra}^{1/3}$, at least to within logarithmic factors [35]. Heat transport is reduced by rotation. This reduction is reproduced in the bound computation, but not by as much as is observed in numerical computations at finite but large Pr. The SDP finds the correct Ra for the onset of convection, but at larger Ra, the bound on Nu increases more rapidly with Ra than the Nu obtained from simulations. The mere fact that momentum equation is reduced to a diagnostic equation is therefore no guarantee that the background method will provide us with satisfactory bounds.

The bounds obtained from the SDP are nonetheless stricter than the bounds obtained from analytical work in as far as the dependence on rotation is concerned. Both types of calculations enforce the same constraints, but the SDP optimizes the background field profile and does not rely on simplifying estimates to ensure the validity of inequalities analogous to (13) usually called spectral constraint in the context of the background method. Linear stability theory computes a critical Rayleigh number Ra_{crit} , which asymptotically scales with Ta as $\text{Ra}_{\text{crit}} \propto \text{Ta}^{2/3}$ at large Ta. For stress-free boundaries, the result from the SDP may be presented as $\text{Nu} \lesssim (\text{Ra}/\text{Ra}_{\text{crit}})^2$ ignoring numerical prefactors. The rotation-dependent bounds obtained analytically are either $\text{Nu} - 1 \lesssim \text{Ra}^{1/2}(\text{Ra}/\text{Ra}_{\text{crit}})^{1/2}$ from Ref. [12] or $\text{Nu} - 1 \lesssim \text{Ra}^{1/2}(\text{Ra}/\text{Ra}_{\text{crit}})^{3/2}$ from Ref. [14] in the rotation-dominated regime. Both of these bounds impose a weaker reduction of Nu with Ta than the bound from the SDP. The expressions for no-slip boundaries are more complicated since the analytical result [14] for the bound on $\text{Nu} - 1$ is a sum of two terms, one varying as $\text{Ra}^{1/2}(\text{Ra}/\text{Ra}_{\text{crit}})^{3/2}$, the other as $\text{Ra}^{5/4}(\text{Ra}/\text{Ra}_{\text{crit}})^{3/4}$. Both terms decrease more slowly with increasing Ta as the $(\text{Ra}/\text{Ra}_{\text{crit}})^\beta$ with $\beta > 2$ in Fig. 2.

The SDP bounds the advective heat flux to zero for $\text{Ra} < \text{Ra}_{\text{crit}}$. The SDP bounds also reflect several qualitative effects known from experiments and numerical simulations, such as a characteristic length scale varying as $\text{Ta}^{-1/6}$ in the rotation-dominated regime. In the case of no-slip boundaries, the heat transport in rapidly rotating convection and in some interval of Rayleigh numbers exceeds the heat transport of nonrotating convection at the same Rayleigh numbers. The exponent β in $\text{Nu} \lesssim (\text{Ra}/\text{Ra}_{\text{crit}})^\beta$ in the bounds for no-slip boundary conditions increases with Ta (see Fig. 2), just as it does in fits to experimentally and numerically determined Nu.

Rotating convection at infinite Prandtl number thus is a system in which significant improvement over existing analytical results is possible within the background method. It is also a system that is a promising testing ground for bounding methods involving additional constraints. It is possible to formulate an SDP, which takes into account more constraints [20], but at the cost of a significantly larger computational burden. A method of this type was recently demonstrated in the context of nonlinear stability analysis [36]. Rotating convection at infinite Prandtl number is a nontrivial fluid dynamic system, which is relatively simple in the sense that it is governed by an equation for a single scalar field, and for which the known bounds do not scale with the control parameters in the

same way as the results of numerical computations, so that this system promises to be particularly rewarding for any improved bounding method.

- [1] E. Hopf, Ein allgemeiner Endlichkeitssatz der Hydrodynamik, *Math. Ann.* **117**, 764 (1941).
- [2] C. R. Doering and P. Constantin, Energy Dissipation in Shear Driven Turbulence, *Phys. Rev. Lett.* **69**, 1648 (1992).
- [3] C. R. Doering and P. Constantin, Variational bounds on energy dissipation in incompressible flows: III. Convection, *Phys. Rev. E* **53**, 5957 (1996).
- [4] G. Fantuzzi, A. Arslan, and A. Wynn, The background method: Theory and computations, *Philos. Trans. R. Soc. London A* **380**, 20210038 (2022).
- [5] W. Malkus, Outline for a theory for turbulent shear flow, *J. Fluid Mech.* **1**, 521 (1956).
- [6] L. Howard, Heat transport by turbulent convection, *J. Fluid Mech.* **17**, 405 (1963).
- [7] F. Busse, On Howard's upper bound for heat transport by turbulent convection, *J. Fluid Mech.* **37**, 457 (1969).
- [8] R. Kerswell, New results in the variational approach to turbulent Boussinesq convection, *Phys. Fluids* **13**, 192 (2001).
- [9] I. Grooms and J. P. Whitehead, Bounds on heat transport in rapidly rotating Rayleigh–Bénard convection, *Nonlinearity* **28**, 29 (2015).
- [10] B. Pachev, J. P. Whitehead, G. Fantuzzi, and I. Grooms, Rigorous bounds on the heat transport of rotating convection with Ekman pumping, *J. Math. Phys.* **61**, 023101 (2020).
- [11] C. Jones, Thermal and compositional convection in the outer core, in *Treatise on Geophysics, 2nd edition*, Vol. 8, edited by G. Schubert (Elsevier, Amsterdam, 2015), pp. 115–159.
- [12] A. Tilgner, Bounds for rotating Rayleigh–Bénard convection at large Prandtl number, *J. Fluid Mech.* **930**, A33 (2022).
- [13] C. Doering and P. Constantin, On upper bounds for infinite Prandtl number convection with or without rotation, *J. Math. Phys.* **42**, 784 (2001).
- [14] P. Constantin, C. Hallstrom, and V. Putkaradze, Heat transport in rotating convection, *Physica D* **125**, 275 (1999).
- [15] N. K. Vitanov, Convective heat transport in a rotating fluid layer of infinite Prandtl number: Optimum fields and upper bound on Nusselt number, *Phys. Rev. E* **67**, 026322 (2003).
- [16] C. Plasting and G. Ierley, Infinite-Prandtl-number convection. Part 1. Conservative bounds, *J. Fluid Mech.* **542**, 343 (2005).
- [17] G. Ierley, R. Kerswell, and C. Plasting, Infinite-Prandtl-number convection. Part 2. A singular limit of upper bound theory, *J. Fluid Mech.* **560**, 159 (2006).
- [18] A. Tilgner, Bounds on poloidal kinetic energy in plane layer convection, *Phys. Rev. Fluids* **2**, 123502 (2017).
- [19] A. Tilgner, Time evolution equation for advective heat transport as a constraint for optimal bounds in Rayleigh–Bénard convection, *Phys. Rev. Fluids* **4**, 014601 (2019).
- [20] S. I. Chernyshenko, P. Goulart, D. Huang, and A. Papachristodoulou, Polynomial sum of squares in fluid dynamics: A review with a look ahead, *Philos. Trans. R. Soc. London A* **372**, 20130350 (2014).
- [21] P. Constantin and C. Doering, Infinite Prandtl number convection, *J. Stat. Phys.* **94**, 159 (1999).
- [22] C. Doering, F. Otto, and M. Reznikoff, Bounds on vertical heat transport for infinite-Prandtl-number Rayleigh–Bénard convection, *J. Fluid Mech.* **560**, 229 (2006).
- [23] F. Otto and C. Seis, Rayleigh–Bénard convection: Improved bounds on the Nusselt number, *J. Math. Phys.* **52**, 083702 (2011).
- [24] S. Chandrasekhar, *Hydrodynamic and Hydromagnetic Stability* (Oxford University Press, Oxford, 1961).
- [25] F. Zhong, R. E. Ecke, and V. Steinberg, Rotating Rayleigh–Bénard convection: asymmetric modes and vortex states, *J. Fluid Mech.* **249**, 135 (1993).

- [26] J.-Q. Zhong, R. J. A. M. Stevens, H. J. H. Clercx, R. Verzicco, D. Lohse, and G. Ahlers, Prandtl-, Rayleigh-, and Rossby-Number Dependence of Heat Transport in Turbulent Rotating Rayleigh-Bénard Convection, *Phys. Rev. Lett.* **102**, 044502 (2009).
- [27] S. Schmitz and A. Tilgner, Transitions in turbulent rotating Rayleigh-Bénard convection, *Geophys. Astrophys. Fluid Dyn.* **104**, 481 (2010).
- [28] S. Schmitz and A. Tilgner, Heat transport in rotating convection without Ekman layers, *Phys. Rev. E* **80**, 015305(R) (2009).
- [29] E. M. King, S. Stellmach, J. Noir, U. Hansen, and J. M. Aurnou, Boundary layer control of rotating convection systems, *Nature (London)* **457**, 301 (2009).
- [30] K. Julien, J. M. Aurnou, M. A. Calkins, E. Knobloch, P. Marti, S. Stellmach, and G. M. Vasil, A nonlinear model for rotationally constrained convection with Ekman pumping, *J. Fluid Mech.* **798**, 50 (2016).
- [31] S. Horn and O. Shishkina, Toroidal and poloidal energy in rotating Rayleigh-Bénard convection, *J. Fluid Mech.* **762**, 232 (2015).
- [32] W. V. R. Malkus and S. Chandrasekhar, The heat transport and spectrum of thermal turbulence, *Proc. R. Soc. London A* **225**, 196 (1954).
- [33] L. N. Howard, Convection at high Rayleigh number, in *Applied Mechanics*, edited by H. Görtler (Springer, Berlin, 1966), pp. 1109–1115.
- [34] S. Chan, Infinite Prandtl number turbulent convection, *Stud. Appl. Math.* **50**, 13 (1971).
- [35] C. Nobili and F. Otto, Limitations of the background field method applied to Rayleigh-Bénard convection, *J. Math. Phys.* **58**, 093102 (2017).
- [36] F. Fuentes, D. Goluskin, and S. Chernyshenko, Global Stability of Fluid Flows Despite Transient Growth of Energy, *Phys. Rev. Lett.* **128**, 204502 (2022).